DOI: 10.1002/chem.200900287

Second-Order Nonlinear Optical Activity of Dipolar Chromophores Based on Pyrrole-Hydrazono Donor Moieties

Alessandro Abbotto,*[a] Luca Beverina,[a] Norberto Manfredi,[a] Giorgio A. Pagani,*[a] Graziano Archetti,[b] Hans-Georg Kuball,[b] Christian Wittenburg,[c] Jürgen Heck,[c] and Jan Holtmann[c]

Dedicated to the memory of Rüdiger Wortmann

Abstract: A series of highly efficient and thermally stable second-order nonlinear optical (NLO) dipolar donor–auxiliary donor–acceptor chromophores have been synthesised in which a hydrazono group and a pyrrole ring act as donor and auxiliary donor components, respectively, in combination with different aromatic and heteroaromatic acceptors. The new dyes have been systematically investigated by NMR spectroscopy, absorption spectroscopy, NLO measurements and thermal stability studies. NLO properties have been studied in detail by electro-optical absorption (EOA) and hyper-Rayleigh scattering (HRS) measurements in 1,4-dioxane and DMSO, respectively. The results originating from the two different methods have been compared and analysed in detail. We found that the NLO properties measured by the EOA and HRS methods correlate with each other and converge to reveal the dye with the acceptor 2-dicyanomethylene-3-cyano-4,5,5-trimethyl-2,5-dihydrofuran as the most efficient system. The unprecedented combination of a strong donor hydrazono group and the auxiliary donor effects of π-excessive heteroaromatic rings afforded NLO chromophores with very high values ($\mu_g\beta_0$(EOA) up to 2038×10^{-48} esu and β(HRS) up to 3980×10^{-30} esu at 1.5 μm).

Keywords: chromophores · electro-optical absorption measurements · heterocycles · hyper-Raleigh scattering · nonlinear optics

Introduction

Dipolar or push–pull chromophores, in which π-conjugated systems are end-capped by donor and acceptor moieties, have been extensively investigated in the last decade for second-order nonlinear optical (NLO) applications in photonic and electro-optic devices, including high-speed photonic switching systems and electro-optic modulators.[1–4] Although a large variety of donor, acceptor and spacer groups have been used for the design of NLOphores, the use of strong donating moieties, such as electron-rich π-excessive heteroaromatic rings,[5] has seldom appeared in the NLO literature.[3a,6] Even more surprisingly is the absence, with very few exceptions,[7,8] of important donor organic functionalities such as hydrazono moieties of the type $R_2N{-}N{=}$, which are able to efficiently delocalise an electron pair residing on the terminal nitrogen atom onto a π-conjugated system.

In recent years we have designed a number of di- and multipolar dyes containing electron-rich and -poor heterocycles as donor and acceptor units.[9,10] In particular, we found that chromophores containing a pyrrole ring as a donor moiety are endowed with remarkable NLO activity. On the basis of INDO/1 semiempirical computations, Ratner et al. predicted in 1997 that the NLO response of dipolar chromophores would be significantly enhanced by interposing π-ex-

---

[a] Prof. Dr. A. Abbotto, Dr. L. Beverina, Dr. N. Manfredi,
Prof. Dr. G. A. Pagani
Department of Materials Science and INSTM
University of Milano-Bicocca
Via Cozzi 53, 20125 Milano (Italy)
Fax: (+39) 02-6448-5400
E-mail: alessandro.abbotto@mater.unimib.it
giorgio.pagani@mater.unimib.it

[b] Dr. G. Archetti, Prof. Dr. H.-G. Kuball
Physikalische Chemie, Technische Universität Kaiserlautern
Erwin-Schrödinger-Str., 67663 Kaiserslautern (Germany)

[c] Dr. C. Wittenburg, Prof. Dr. J. Heck, J. Holtmann
Institut fürAnorganische und Angewandte Chemie
Universität Hamburg
Martin-Luther-King Platz 6, 20146 Hamburg (Germany)

Supporting information for this article is available on the WWW under http://dx.doi.org/10.1002/chem.200900287.

cessive or -deficient heterocyclic bridges between strong donor or acceptor groups.[11] The auxiliary donor effect, generally larger than the auxiliary acceptor effect, is predicted to be particularly strong for the electron-rich pyrrole ring. More recently, the pyrrole ring was incorporated as an auxiliary donor into efficient dipolar chromophores with two-photon absorption activity.[12]

Encouraged by the aforementioned predicted NLO enhancement by the auxiliary donor effect, we reasoned that the presence of a strong electron-donating group such as a terminal amino functionality directly attached to the electron-donating auxiliary moiety would be highly beneficial in terms of enhancing the second-order NLO performance. It is well known, however, that amino-functionalised π-excessive heterocycles (furan, thiophene and pyrrole) have limited synthetic access and once prepared are endowed with poor thermal stability because of easy oxidative degradation. Thus, we turned to the vinylogy concept and, in particular, aza-vinylogy. We considered that hydrazones are azavinylogues[13] of amino functionalities. Phenyl- and diphenylhydrazones are consequently viewed as phenyl- and diphenylamino azavinylogues, the donor moiety being the phenyl- and diphenylamino group. We decided to investigate the second-order NLO molecular properties of a class of dipolar chromophores combining the following design elements: 1) differently substituted hydrazono moieties as strong donor moieties in dipolar dyes; 2) the pyrrole ring as a co-donor (or auxiliary donor) unit and 3) strong acceptor groups. Some of us have previously described the large electro-optic responses of hydrazono derivatives carrying a pyrrole ring as co-donor and a pyridine ring as acceptor in hydrogen-bonded films grown by physical vapour deposition.[8] We selected three different acceptor moieties on the basis of their efficiency and stability in NLO applications: the pyridinium group, a very common group in stilbazolium and other efficient NLO derivatives,[2,9] 2,4-dinitrophenyl,[14] and 2-dicyanomethylene-3-cyano-4,5,5-trimethyl-2,5-dihydrofuran,[15] successfully embedded in a number of NLO chromophores with exceptionally large β values.[2,16]

We herein describe the synthesis, optical and nonlinear optical characterisation and thermal stability of the new hydrazono chromophores **1a**, **2a** and **1b**–**3b**. The two sets of dyes **a** and **b** carry a different substitution pattern on the terminal hydrazono moiety, that is, monophenyl- (**a**) versus diphenylhydrazono (**b**) derivatives, to enable the effect of tuning of the donor properties on the NLO properties to be investigated.

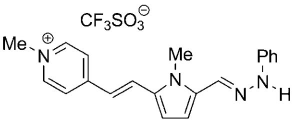

1a

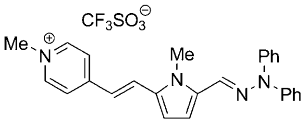

1b

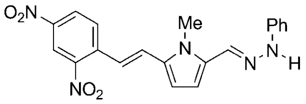

2a

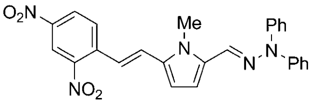

2b

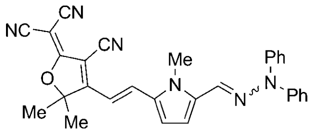

3b

Results and Discussion

Synthesis: Mono- and diphenylhydrazonopyrrole derivatives carrying a terminal acceptor moiety have been scantly reported in the literature.[8] The previously unknown dyes **1**–**3** were synthesised following the two different general routes depicted in Scheme 1. Route A is based on the Vilsmeier–Haack formylation of the push–pull ethene derivative **5** and the final condensation of **6** with phenylhydrazine or diphenylhydrazine. This route cannot be applied to the synthesis of chromophore **3b** due to the strong accepting properties of the tricyanofuran moiety, which deactivates the pyrrole

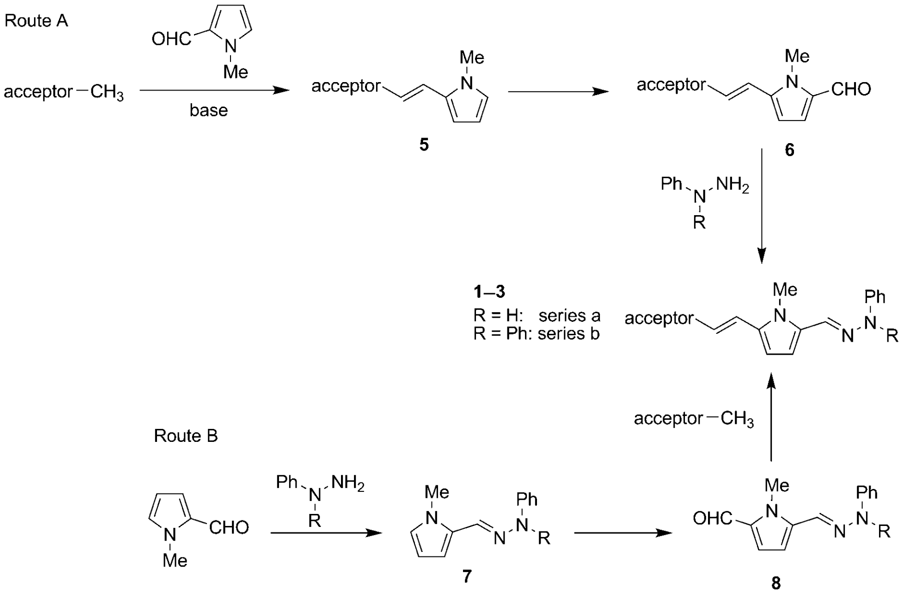

Scheme 1.

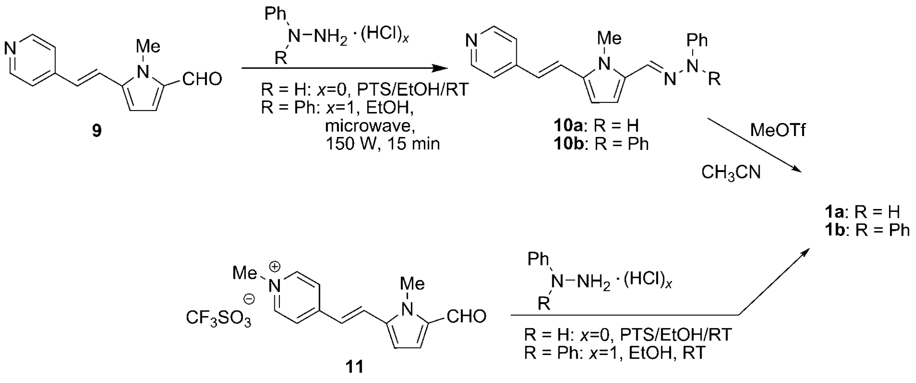

Scheme 2.

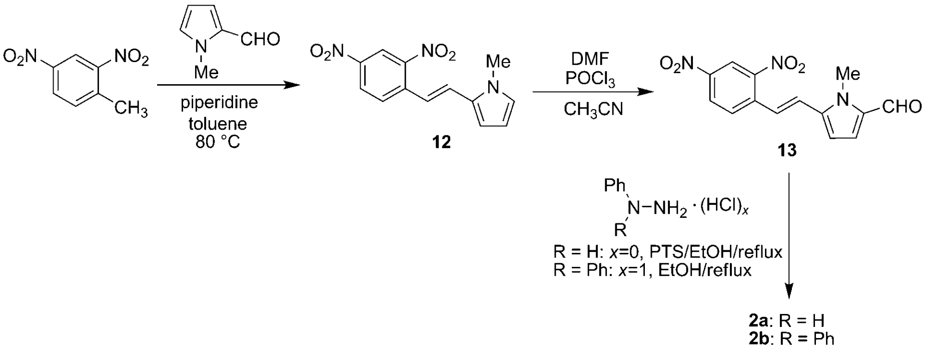

Scheme 3.

ring towards the Vilsmeier–Haack formylation and thus inhibits the formation of **6**. We have therefore envisaged the alternative Route B, which involves formylation of the 5-position of the pyrrolyl ring of the hydrazone **7** of *N*-methyl-2-pyrrolecarbaldehyde and condensation to introduce the acceptor group.

Route A (Scheme 1) was applied to the synthesis of the pyridinium derivatives **1a** and **1b** and the dinitrophenyl derivatives **2a** and **2b**, according to Schemes 2 and 3, respectively. Acid-catalysed or microwave-promoted condensation of aldehyde **9**[10c] with diphenyl- or phenylhydrazine gave the corresponding hydrazones **10a** and **10b**. Final alkylation with methyl triflate afforded the products **1a** and **1b**. Alternatively, the hydrazones were formed from the quaternised pyridinium precursor **11**[10b] directly generating chromophores **1a** and **1b**. Similarly, formylation of the ethene derivative **12** and condensation of the resulting aldehyde **13** with the appropriate arylhydrazine yielded dyes **2a** and **2b**.

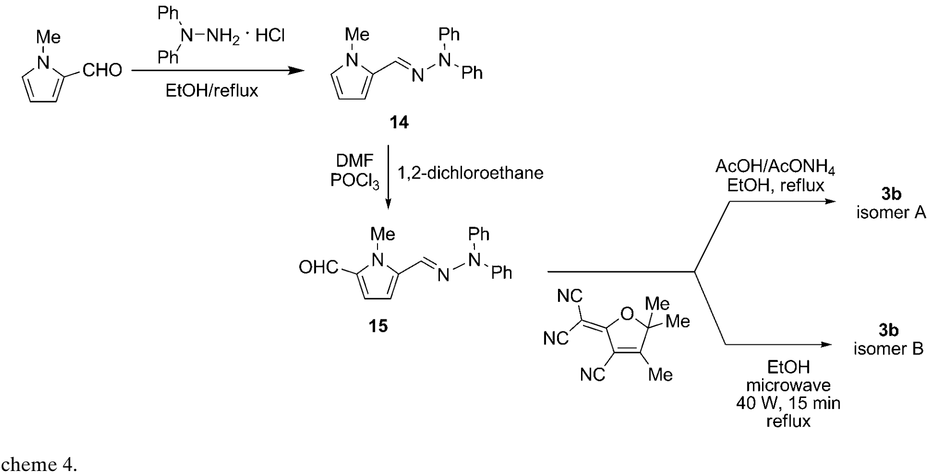

Scheme 4.

Chromophore **3b** was obtained by Route B (Scheme 1) according to Scheme 4. Diphenylhydrazone **14**[17] was submitted to Vilsmeier–Haack formylation to give the corresponding aldehyde **15**. Unfortunately, formylation of the monophenylhydrazone derivative **7** (R=H) gave the *N*-formyl product, which prevented the formation of the monophenylhydrazone chromophore **3a**. Acid-catalysed condensation of **15** with 3-cyano-2-dicyanomethylene-4,5,5-trimethyl-2,5-dihydrofuran[16f] afforded the chromophore **3b** (isomer A) in good yield. However, when base-free microwave-assisted condensation was performed a different isomer of **3b** (isomer B) was isolated. NMR spectroscopy, mass spectrometry and UV/Vis spectroscopy analysis suggested that isomers A and B are likely to be *E* and *Z* stereoisomers around the C=N hydrazone bond, respectively. All of the new dyes were characterised by NMR spectroscopy and high-resolution mass spectrometry. Selected ^{1}H NMR chemical shifts of dyes **1a**, **2a** and **1b**–**3b** are collected in Table 1.

The ^{1}H NMR spectra of mono- and diphenylhydrazono derivatives carrying the same acceptor group are rather similar to each other. The most apparent difference is the chemical shift of the olefin proton bound to the carbon–nitrogen hydrazone bond, which is centred around $\delta = 7.9$ ppm in the monophenylhydrazono dyes and around $\delta = 7.0$–7.3 ppm in their diphenylhydrazono counterparts. This effect

Table 1. Selected ^1H NMR chemical shifts [ppm] of chromophores **1a**, **2a** and **1b**–**3b** in DMSO.[a]

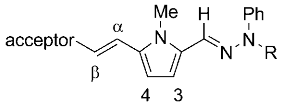

Compound	α	β	3	4	H−C=N−
1a	7.94	7.13	6.61	6.99	7.90
	(15.7)	(15.7)	(4.2)	(4.2)	
2a	7.70	7.27	6.53	6.83	7.88
	(15.7)	(15.7)	(4.2)	(4.1)	
1b	7.96	7.15[b]	6.55	6.97	7.15
	(15.7)		(4.2)	(4.2)	
2b	7.60	7.17	6.36	6.70	7.04
	(15.5)	(15.5)	(4.2)	(4.2)	
(*E*)-**3b** (isomer A)	7.99	6.86	6.84	7.53	7.16
	(15.5)	(15.5)	(4.7)	(4.7)	
(*Z*)-**3b** (isomer B)	7.86	6.73	6.84	7.12	7.32
	(15.5)	(15.5)	(2.8)	(2.8)	

[a] Coupling constants in parentheses [Hz]. [b] Mean value of a multiplet corresponding to six protons.

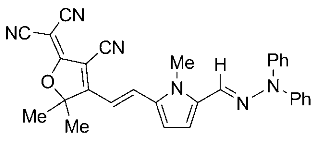

E-**3b**
(isomer A)

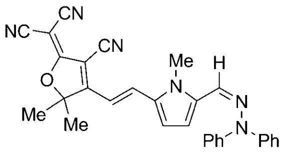

Z-**3b**
(isomer B)

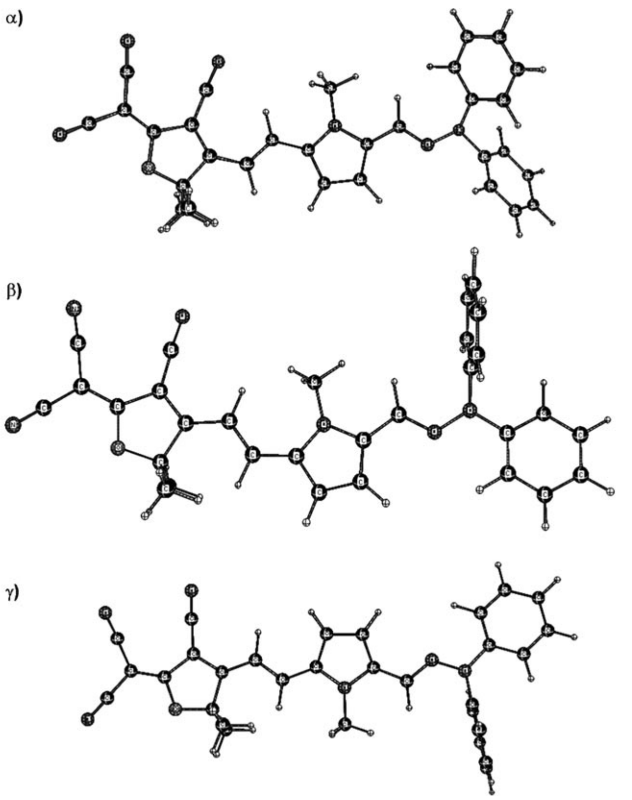

Figure 1. PM3-optimised structures of (*E*)-**3b** (isomer A) (energies of optimised structures of conformers α, β and γ differ by less than 0.5 kcal mol^{-1}).

is likely to be due to the shielding effect of two versus one phenyl ring bound to the terminal nitrogen atom of the hydrazono moiety. In addition, the NMR spectra of the monophenylhydrazono derivatives are characterised by the presence of a singlet at around $\delta = 10$ ppm, assigned to the NH proton of the hydrazono moiety. Rather unexpectedly, ethene and pyrrole protons are shifted upfield, though very slightly, on going from the mono- to the corresponding diphenylhydrazono derivatives, which suggests a somewhat stronger donor capacity of the diphenylhydrazono compared with the monophenylhydrazono moiety. This result is in contrast to the hypothesis that the presence of two phenyl rings in place of one should make the electron pair on the terminal nitrogen atom less available for delocalisation onto the π framework. In agreement with the NMR spectroscopy results, the PM3-optimised structures of **3b** (Figure 1) show that the two phenyl rings of the diphenylhydrazono moiety are not coplanar with the π framework of the rest of the molecule, thus the adjacent nitrogen electron pair is delocalised less efficiently onto the phenyl rings and allows preferential delocalisation onto the pyrrole ring. Recent electron-donor strength studies of aromatic amines have established that, because of steric effects, the diphenylamino group is a poorer π donor than dialkylamino when directly bonded to an aromatic π framework.[18] Our finding, in apparent contrast, that diphenylamino behaves as a stronger donor than monophenylamino can be explained by the presence of a C=N spacer between the donor and the remaining π framework, thus bypassing group hindrance.

As expected, larger differences are recorded by varying the acceptor moiety. The effect of the acceptor end group on the ^1H NMR chemical shifts is evident both for the ethenyl and the pyrrolyl positions. Analysis of the chemical shifts in the series **1b**–**3b** shows that positions in compounds **1b** and **3b** are shifted downfield with respect to **2b**, which confirms that the pyridinium and the dihydrofuran moieties are stronger acceptors than the dinitrophenyl group. This conclusion is particularly evident for the ethenyl α position and the pyrrolyl 4-position, which are the two sites in direct conjugation (positively charged sites in resonance structures) with the acceptor group.

Comparison of the ^1H NMR spectra of the two isomers of **3b** is useful to obtain some insights into their structures. The two ^1H (Figure 2) and ^{13}C NMR (see the Supporting Information) spectra are very similar to each other. The ethenyl and pyrrolyl ^1H chemical shifts of isomer B are shifted slightly upfield with respect to isomer A. This result is consistent with a higher donor capacity of the diphenylhydrazono end group in isomer B compared with isomer A. Therefore, we hypothesise that the two isomers are likely to be the *E* (isomer A) and *Z* (isomer B) geometrical isomers of **3b** around the hydrazone π bond. The identical values of the vicinal coupling constants of the ethene bridge adjacent to the acceptor group rule out the hypothesis that geometri-

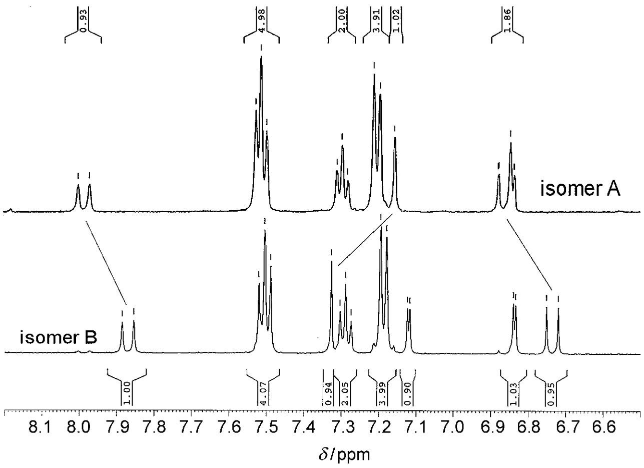

Figure 2. Comparison of ^1H NMR spectra of the ethenylic and aromatic region of **3b** (isomer A) and **3b** (isomer B) (main differences are outlined).

cal isomerism involves this double bond. The existence of the two isomers is supported by the analysis of the chemical shifts of the methine proton bound to the carbon–nitrogen hydrazone bond ($\delta = 7.16$ and 7.32 ppm in isomers A and B, respectively). Indeed, the shielding effect of the two phenyl rings is expected to be less efficient in the *Z* isomer than in the *E* isomer.

Linear optical properties: The compounds **1a**, **2a** and **1b**–**3b** present an intense transition in the visible region of their UV/Vis spectra. The absorption data for this band are collected in Table 2 for selected solvents. Figure 3a shows the absorption spectra of compound (*Z*)-**3b** in five solvents of different polarity ($\varepsilon_r = 2.21$–46.7) and Figure 3b compares the spectra of compounds **2b**, (*E*)-**3b** and (*Z*)-**3b** in 1,4-dioxane (the spectra in DMSO are available in the Supporting Information). All the chromophores show a positive solvatochromism in their low-energy absorption band, which indicates that the dipole moment in the excited state is larger than in the ground state (Table 2).[19,20] The size of the solvatochromism suggests that the long-wavelength band possesses charge-transfer (CT) character.

Table 2. Solvatochromism of the CT band (λ_{max} [nm]) for the chromophores **1a**, **2a** and **1b**–**3b** in selected solvents (polarity index is reported in brackets).

Compound	Dioxane (4.8)	$CHCl_3$ (4.1)	EtOH (5.2)	DMF (6.4)	DMSO (7.2)	$\Delta\nu$ [cm^{-1}][a]
1a	522	564	559	538	539	1427
1b	538	578	546	528	528	1286
2a	529	538	519	545	554	316
2b	528	558	518	540	548	1018
(*E*)-**3b** (isomer A)	629	660	652	652	656	772
(*Z*)-**3b** (isomer B)	568	597	605	590	596	855

[a] $\Delta\nu = \nu(\text{dioxane}) - \nu(CHCl_3)$.

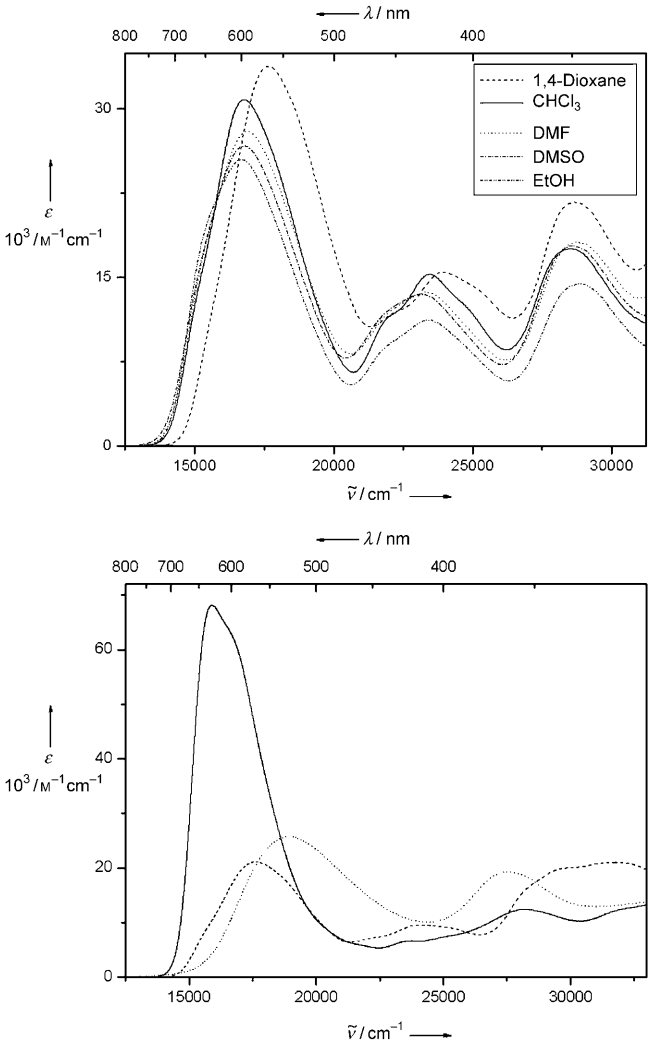

Figure 3. a) UV/Vis spectra of (*Z*)-**3b** in different solvents. b) UV/Vis absorption spectra of **2b** (•••••), (*Z*)-**3b** (-----) and (*E*)-**3b** (——) in 1,4-dioxane ($T = 298$ K, ca. 10^{-5} M). Compound **1b** was not soluble enough in 1,4-dioxane to obtain the corresponding molar extinction coefficient.

Some important insights can be derived by comparing the spectral position of the CT band as the acceptor or the donor end group is varied. This absorption band is bathochromically shifted on going from chromophores **1** and **2** to **3b**. The larger bathochromic effect of the tricyanodihydrofuran group compared with the other two acceptors is likely to be the consequence of the stronger electron-withdrawing strength of the former, which enhances the intramolecular charge transfer from the donor end group. Furthermore, by using the tricyanodihydrofuran moiety as an acceptor group an additional shoulder appears in the CT band, which suggests the existence of overlapping transitions.

The effect of the donor monophenyl- versus diphenylhydrazono group (series **a** vs. series **b**) depends on the solvent polarity. For solvents of low polarity (dioxane, $CHCl_3$) the spectral band position of the diphenylhydrazono derivative **1b** is shifted to lower energies with respect to the monophenylhydrazono counterpart **1a**. However, with the exception of **2** in $CHCl_3$, the band position of **2a** is always lower in energy than that of **2b**. The reason for such behaviour is not obvious, but it clearly suggests a strong perturbation of the electronic structures of the chromophores and an influence of the conformational distribution, as shown in Figure 1.

Some other insights into the effect of the configurational change for **3b** become evident by comparing the shapes and spectral positions of the CT bands of the *E* and *Z* isomers (Table 2, Figure 3). Firstly, the shoulder appears in different positions: At a lower energy for (*Z*)-**3b** and at a higher energy for (*E*)-**3b** with respect to the CT absorption maximum. Secondly, the maximum of the CT band of (*Z*)-**3b** is always hypsochromically shifted by around 60 nm compared with (*E*)-**3b**, regardless of solvent polarity.

Nonlinear optical properties: Second-order molecular NLO properties have been investigated by electro-optical absorption (EOA)[21,22] and hyper-Rayleigh scattering (HRS) measurements in 1,4-dioxane and DMSO, respectively.

EOA Measurements: EOA spectroscopy is a suitable method for obtaining dipole moments of the ground (μ_g) and excited (μ_e) electronic states and allows for the evaluation of (hyper)polarisabilities of uniformly polarised absorption band of a single compound in a dilute solution in an electric field *E*. Experimentally the very small absorption difference $\varepsilon^E(\phi,\tilde{\nu})-\varepsilon(\tilde{\nu})$ is measured with light linearly polarised parallel ($\phi=0°$) and perpendicular ($\phi=90°$) to **E** as a function of the wavenumber $\tilde{\nu}$ [Eq. (1)]. $\varepsilon^E(\phi,\tilde{\nu})$ and $\varepsilon(\phi,\tilde{\nu})$ are the molar decadic absorption coefficients of the solution in the presence and in the absence of the externally applied electric field, respectively.

$$L(\varphi,\tilde{\nu}) = \frac{\varepsilon^E(\varphi,\tilde{\nu}) - \varepsilon(\tilde{\nu})}{\varepsilon(\tilde{\nu})}\frac{1}{E^2} \tag{1}$$

The EOA spectra of compounds **2a**, **2b**, (*E*)-**3b** and (*Z*)-**3b** are shown in Figure 4 and the Supporting Information. Owing to the applied strong electric field needed for the measurements, EOA spectra cannot be recorded for salt-like derivatives such as **1**.

The EOA spectrum $L(\phi,\tilde{\nu})\varepsilon(\tilde{\nu})\tilde{\nu}^{-1}$ is determined by three effects: the electrodichroic effect, the Stark effect and the field dependence of the transition dipole moment. The electrodichroic effect is the dependence of the intensity of absorption for differently polarised light originated by the induced orientational order of the molecules in the electric field, modified by the field dependence of the absorption coefficient. The electrodichroism is positive (negative) when the absorption in the electric field increases (decreases) for parallel ($\varphi=0°$) and decreases (increases) for perpendicular ($\varphi=90°$) detection in comparison with the isotropic solution. The Stark effect is the shift of the absorption band in the presence of the electric field, which only occurs when the optical excitation is accompanied by a change in the dipole moment ($\Delta\mu=\mu_e-\mu_g$). A bathochromic (hypsochromic) shift relative to the isotropic absorption spectrum is due to an increase (a decrease) in the molecular dipole moment on going from the ground to the excited state ($\Delta\mu>0$ and $\Delta\mu<0$, respectively).

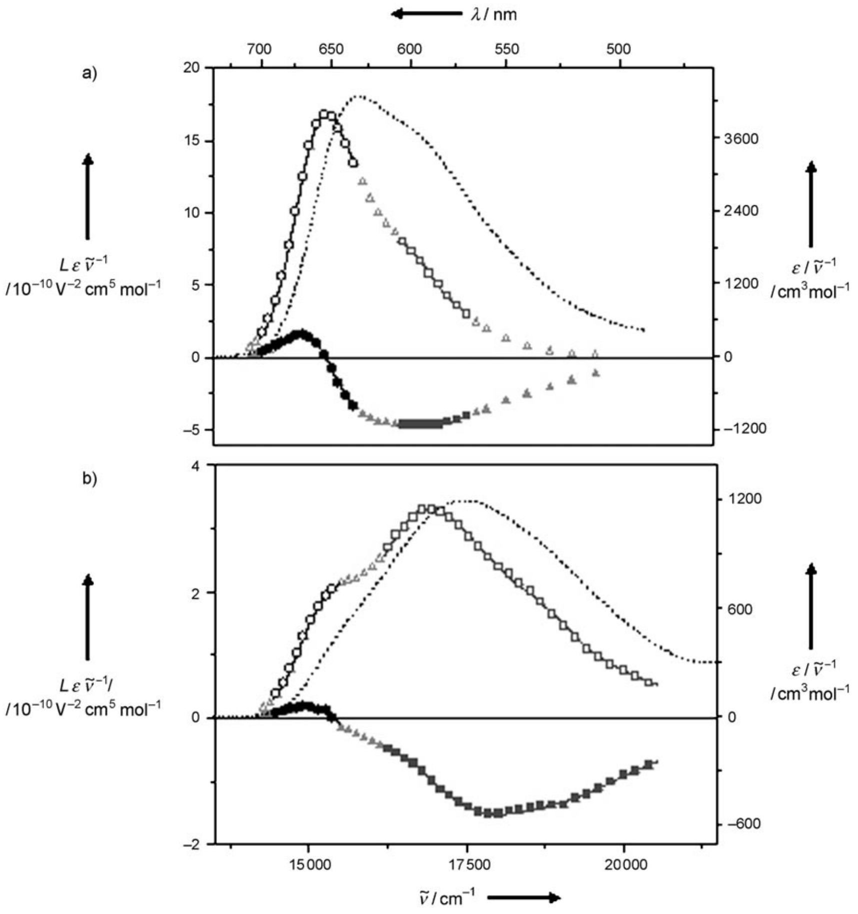

Figure 4. Fitted EOA spectra (solid lines, left scale) at 298 K in 1,4-dioxane for (*E*)-**3b** (a) and (*Z*)-**3b** (b). The open symbols (○,△,□) show the measured change of absorption for light polarised parallel to the electric field. The filled symbols (●,▲,■) depict the change of absorption for light polarised perpendicular to the electrical field. Open and full circles and squares have been used to indicate the first and second bands, respectively, in the different spectral regions used for two independent fits. For comparison, the UV/Vis absorption spectrum is also shown (dashed lines, right scale).

From the multilinear regression coefficients D to H (see the Experimental Section and the Supporting Information) the dipole moment of the ground state μ_g and the dipole moment difference $\Delta\mu$ for **2a** and **2b** were calculated under the assumption that the electronic transition/transitions (μ_{eg}) are polarised parallel to the dipole moments. This is not true for (E)-**3b** and (Z)-**3b**. In particular, for (Z)-**3b** the EOA measurements show that there are two differently polarised transitions superposed for which the electric dipole moment and the transition moment are oriented differently ($Q \neq 1$, see the Supporting Information). Whereas the dipole differences $\Delta\mu$ were calculated from the average values of the regression coefficients F and G, the ground-state dipole moment μ_g was obtained from the difference $E-6D$.[23] Solvent effects were corrected by local fields within the approximations of Onsager's continuum model.[24] The dipole moments of **2** and **3** increase with the polarity of the solvent, that is, about 20–30 % in 1,4-dioxane solution (see the Supporting Information). Polarisability effects were neglected in 1,4-dioxane. The results of the EOA analysis are collected in Table 3.

Table 3. UV/Vis and EOAM data[a] of **2a**, **2b** and **3b** in 1,4-dioxane.

Compound	λ_{eg} [nm]	μ_{eg} [D]	Fitting range [nm]	μg[a] [D]	$\Delta\mu$ [D]
2a	528.5	8.2	640–480	5.6 ± 0.1	27.3 ± 1.4
2b	527.7	8.4	620–500	5.9 ± 0.1	31.2 ± 1.4
(E)-**3b**	628.6	11.2	700–635	13.0 ± 0.1	10.8 ± 0.4
			605–570	13.1 ± 0.1	14.2 ± 0.5
(Z)-**3b**	568.0	6.7	700–645	12.9 ± 0.1	11.6 ± 0.2
			615–490	13.0 ± 0.1	10.3 ± 1.1

[a] Measurements have been performed in 1,4-dioxane at a concentration of about 10^{-5} M at 298 K. The solvent effect has been corrected within the Onsager's continuum model.

All the chromophores show positive electrodichroism and high values of $\Delta\mu$. The latter confirms the CT character of the lowest-energy transitions. The ground-state dipole moment in 1,4-dioxane more than doubles by moving from the dinitrophenyl acceptor to the tricyanodihydrofuran moiety, whereas the dipole difference $\Delta\mu$ becomes much smaller. This finding is consistent with the hypothesis that the extent of the charge transfer in their ground states is higher for derivative **3b** than for **2a** and **2b**. The effect of the monophenylamino donor compared with the diphenylamino donor group was found to slightly affect the ground-state dipole moment, in agreement with the results of the NMR spectroscopy analysis. Compound **2b** has an excited-state dipole moment 4 debye higher than **2a**, which could also be an effect of the stronger donor character of the diphenylamino group. The solvatochromism for compounds **2** and **3** (Table 2) is consistent with the approximately equal product $\mu_g\Delta\mu$ (Table 3) derived from the EOA spectra.

As is already clear from the UV/Vis spectra (Figure 3), the EOA spectra of (E)-**3b** and (Z)-**3b** (Figure 4) are a result of the contribution of at least two overlapping transitions. To apply Equation (1), a multilinear fitting analysis was performed in two different frequency ranges (ca. 14300–15600 cm^{-1} and 16400–18900 cm^{-1}), in which the contribution from two overlapping bands was found not to be significant.

The dipole moments obtained from the two overlapping bands are identical for (E)-**3b** and (Z)-**3b** within experimental error. This suggests that the bands must belong to the same molecule and not to two different species. There are two possible explanations for these bands: 1) different excited states are reached upon electronic excitation and 2) the two transitions have a vibronic origin. The differences in the dipole changes of the Franck–Condon excited states belonging to the two overlapping bands of the two isomers ($\Delta\Delta\mu =$ 3.4 and 1.3 debye for (E)-**3b** and (Z)-**3b**, respectively; see Table 3) is probably too large to be of vibronic origin. Unexpectedly, (E)-**3b** and (Z)-**3b** also possess the same ground-state dipole moment, which is a restriction to the conclusion discussed before. On the other hand, the nonparallel oriented transition dipole moment and dipole moments are consistent with the assumption of a Z conformer.

Within the assumption of a one-dimensional chromophore,[25] the static hyperpolarisability tensor coordinate along the direction μ_g can be calculated according to the two-level model [Eq. (2)] by using the Taylor (T) or the phenomenological convention (X).[20,22,26]

$$\beta(00,0) = \beta_0 = \frac{6(\mu_{eg}\lambda_{eg})^2 \Delta\mu}{(hc)^2} \tag{2}$$

The β_0 values for **2a**, **2b**, (E)-**3b** and (Z)-**3b** are collected in Table 4. Since the transition dipole moment for each single overlapping transition of **3b** is not known, for the calculation of β_0 the average value of $\Delta\mu$ (Table 3) was used and assumed that for (E)-**3b** and (Z)-**3b** a Two-Level Model can be applied. According to the figure-of-merit $\mu_g\beta_0$, the most promising chromophore for non-linear optical applications is **3b** in its E form, while the less efficient one is **3b** in its Z form.

Table 4. First hyperpolarisabilities and product $\mu_g\beta_0$ for the chromophores **1a**, **2a** and **1b**–**3b** from EOA (in dioxane) and HRS (in DMSO) measurements. All data are solvent corrected by equations derived from continuum theory.[a] EOA and HRS data have been converted to the phenomenological convention (X convention).[25]

	EOA measurements		HRS measurements	
Compound	$\beta_0/10^{-30}$ [esu]	$\mu_g\beta_0/10^{-48}$ [esu]	β@1.5 μm/10^{-30} [esu]	$\beta_0/10^{-30}$ [esu]
1a	[b]	[b]	[c]	[c]
2a	161	723	low[d]	low[d]
1b	[b]	[b]	[c]	[c]
2b	197	932	203	89
(E)-**3b** (isomer A)	194	2038	3980	757
(Z)-**3b** (isomer B)	49	510	720	224

[a] See Table S2 in the Supporting Information and references cited therein. [b] Salts cannot be investigated by the EOA technique due to the presence of the strong external electric field. [c] HRS measurements are not feasible due to strong dye fluorescence. [d] Signal is slightly above the detection limit of approximately 40.

HRS measurements of the first hyperpolarisabilities: The measurements at a wavelength of 1500 nm were carried out as previously described.[27] Instead of the third harmonic (355 nm) generated from an Nd:YAG laser with a wavelength of 1064 nm, the optical parametric oscillator (OPO)[28] in use was pumped with the second harmonic (532 nm). The signal intensity at 824 nm and the fundamental at 532 nm were removed from the Idler using dichroic mirrors, a green-light filter (HR 532) and a silicon filter (HR 650–850; transparent > 1000 nm). An additional Glan-Taylor polariser ensured the vertical polarisation of the beam into the measurement cell. Measurements were performed with 10^{-4}–10^{-6} M solutions. UV/Vis measurements displayed a linear correlation between extinction and concentration according to Lambert–Beer's Law. Disperse Red 1 (DR1) was used as an external standard. The hyperpolarisability was obtained by comparing the slopes of the reference in $CHCl_3$ and DMSO to obtain the ratio of β_{solute}.[29] By using the value of $\beta(CHCl_3) = 80\times10^{-30}$ esu[30], the hyperpolarisability of DR1 in DMSO is estimated to be 253×10^{-30} esu. Interference filters with a bandwidth of 2 nm were used to ensure that only the frequency doubled radiation at 750 nm was detected. The absence of fluorescence radiation was checked by the use of interference filters at 700 nm. The effect of the refractive indices of the solvents was corrected by using the simple Lorentz local field.[31] Experimental static optical first hyperpolarisability β_0 values of HRS are collected in Table 4 and compared with the results of the EOA spectroscopy.

The hyperpolarisability calculated from the EOA is the contribution of the long-wavelength CT band to the static β_0, which corresponds to the HRS extrapolated to $\omega = 0$. In spite of the fact that the contribution of the long-wavelength CT band is by far the largest contribution from all transitions in the short wavelength region, one has to expect that these values are normally distinctly smaller than the HRS results. Because the ratios of the β_0 values of the (*E*)-**3b** and (*Z*)-**3b** isomers are consistent, the HRS as well as the EOA results reflect the NLO efficiency of the synthesised compounds. The efficiencies of **2a** and **2b** obtained from EOA are of the same size as for (*E*)-**3b** (Table 4). Their figures of merit are smaller than those of (*E*)-**3b** because the smaller dipole moments and their larger $\Delta\mu$ do not compensate the smaller intensity of absorption. The low HRS signal suggests that the contributions of the higher absorption bands are smaller in **2a** and **2b** than in (*E*)-**3b** and, thus, the contribution of the CT band completely determines the static β_0.

Thermal stability: Thermal stability of chromophores **1b**–**3b** was checked by isothermal heating in the air of host–guest polysulfone films doped with 50 wt % of chromophore. Relative degradation of host–guest films as a function of temperature is depicted in Figure 5. It is evident that thermal stability is strongly dependent on the nature of the acceptor moiety. Both isomers **3b**, carrying the tricyano-dihydrofuran group, are found to be much more stable than the pyridinium and dinitrophenyl derivatives. Thermal degradation of both isomers of **3b** is less than 20 % at 200 °C, to be compared with a 70 % degradation or more of the other compounds. Chromophore (*Z*)-**3b** is the most stable compound, with no significant degradation up to 160 °C. The stability is expected to be significantly improved when the NLOphores are incorporated in a device-type structure by operating in an inert gas atmosphere.[16e] This result clearly suggests that the two dyes **3b** are the best candidates to successfully withstand poling conditions without significant degradation.[32]

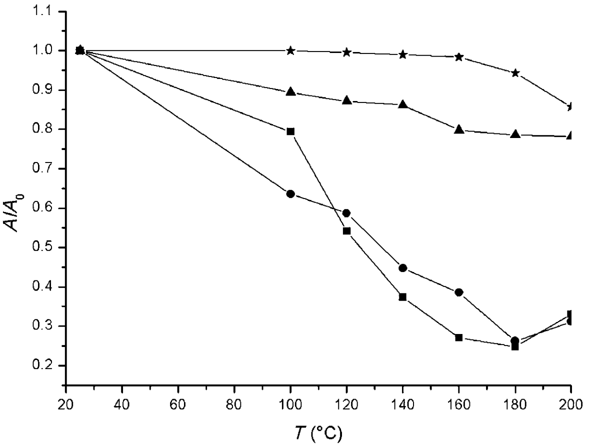

Figure 5. Temperature-dependent degradation in air of chromophores **1b** (●), **2b** (■) and **3b** isomers A (▲) and B (★) in host–guest polysulfone films in terms of decreasing of absorption after thermal treatment (*A*) with respect to starting value (A_0).

Conclusions

A combination of organic design and synthesis, NMR investigation, computations, optical absorption spectroscopy, EOA and HRS measurements of NLO properties and thermal stability has been applied to the investigation of a new family of dipolar donor–acceptor compounds based on pyrrole-hydrazono donor end groups. Different acceptor groups have been embedded in the dipolar structure to study the effect on linear and nonlinear optical properties. Despite the huge number of dipolar compounds showing NLO activity reported in the literature, the concept of combining the donor properties of the hydrazono group and the auxiliary donor effects of electron-rich heteroaromatic rings is unprecedented in the literature, giving rise to the novel family of NLOphores herein described.

Indeed, this multidisciplinary study has demonstrated that this class of chromophores is endowed with good to large second-order molecular NLO activity. The hyperpolarisabilities determined by EOA originate from the contribution of long-wavelength CT absorption, whereas the total hyperpolarisability is obtained as an elastic quantity by the HRS approach. In many cases such long-wavelength CT band gives the dominating contribution to the static hyperpolarisability in comparison to the effect of all other transitions from the shorter wavelength region. Then, the NLO properties measured by the EOA and HRS investigation correlate to each other as previously experimentally shown by Wortmann and Goebel.[33] The different solvents may also account for the deviations in the two types of measurements. Both methods show that chromophore (*E*)-**3b** has the largest NLO activity in the series.

The new efficient NLOphore combines three strategically important design contributions: 1) the use of diphenylhydrazono as an efficient donor group; 2) the use of 2-dicyanomethylene-3-cyano-4,5,5-trimethyl-2,5-dihydrofuran as efficient acceptor groups; 3) the use of the electron-rich pyrrole ring as an efficient auxiliary donor spacer. The three subunits are also combined in the isomer (*Z*)-**3b**, but in this case the NLO activity is approximately four-fold smaller, as measured by both EOA and HRS studies, which is likely to be due to the effect of the *cis* double-bond arrangement on the π-conjugated framework. The first hyperpolarisability of compound (*E*)-**3b** is very promising for its use in electro-optical devices. Investigation of bulk NLO properties of polymeric and sol–gel host–guest and side-chain materials based on the most performing chromophores of this series is in progress.

Experimental Section

General: ^{1}H NMR coupling constants are presented in Hertz. Extracts were dried over Na_2SO_4. Anhydrous DMF was supplied by FLUKA and stored over molecular sieves. Anhydrous acetonitrile was supplied by Aldrich and stored under nitrogen. All other commercial chemicals were supplied by Aldrich and used without purification. Melting points are uncorrected. NMR spectra were recorded with a Bruker 500 MHz spectrometer. UV/Vis spectra were performed with a Jasco V570 spectrophotometer at room temperature. HR-ESIMS were carried out using a Bruker ICR-FTMS Apex II spectrometer.

***N*-Methyl-2-(*N*-phenylhydrazonomethyl)-5-[2-(pyrid-4-yl)vinyl]pyrrole (10a)**: A solution of *N*-phenylhydrazine (0.330 g, 3.07 mmol) in EtOH (5 mL) was added dropwise to a mixture of aldehyde **9**[10c] (0.650 g, 3.07 mmol) and *p*-toluenesulfonic acid (0.530 g, 3.07 mmol) in EtOH (50 mL). After stirring for 3 days at room temperature the deep-red precipitate was collected by filtration. A solution of the precipitate in AcOEt (200 mL) was filtered through basic Amberlite. The solvent was evaporated under reduced pressure to give the product as a red-orange solid (0.461 g, 1.52 mmol, 50 %). M.p. 168 °C; ^{1}H NMR (500 MHz, [D$_6$]DMSO): $\delta = 10.10$ (s, 1H), 8.50 (d, $J = 6.0$ Hz,2H), 7.87 (s, 1H), 7.55 (d, $J = 6.0$ Hz, 2H), 7.53 (d, $J = 16.5$ Hz, 1H), 7.22 (t, $J = 7.8$ Hz, 2H), 6.99 (d, $J = 8.0$ Hz, 2H), 6.98 (d, $J = 16.5$ Hz, 1H), 6.74 (d, $J = 4.5$ Hz, 1H), 6.73 (t, $J = 7.3$ Hz, 1H), 6.45 (d, $J = 4.1$ Hz, 1H), 4.00 ppm (s, 3H); HR-ESIMS: *m*/*z* calcd for $C_{19}H_{19}N_4$: 303.16097 $[M+H]^+$, 325.14292 $[M+Na]^+$; found: 303.16048, 325.14240.

***N*-Methyl-2-(*N*-phenylhydrazonomethyl)-5-[2-(*N*-methylpyrid-4-yl)vinyl]-pyrrole triflate (1a)**

Method A: A solution of methyl triflate (0.172 g, 1.06 mmol) in anhydrous CH_3CN (5 mL) was added dropwise to a solution of **10a** (0.320 g, 1.06 mmol) in the same solvent (45 mL). After stirring overnight the solvent was evaporated under reduced pressure to leave a solid that was dissolved in EtOH (10 mL) to give the product as a dark violet solid (0.359 g, 0.77 mmol, 73 %). M.p. 178 °C; ^{1}H NMR (500 MHz, [D$_6$]DMSO): $\delta = 10.46$ (s, 1H), 8.65 (d, $J = 6.7$ Hz, 2H), 8.08 (d, $J = 6.7$ Hz, 2H), 7.94 (d, $J = 15.7$ Hz, 1H), 7.90 (s, 1H), 7.21 (t, $J = 7.8$ Hz, 2H), 7.13 (d, $J = 15.7$ Hz, 1H), 7.01 (d, $J = 8.0$ Hz, 2H), 6.99 (d, $J = 4.2$ Hz, 1H), 6.77 (t, $J = 7.3$ Hz, 1H), 6.61 (d, $J = 4.2$ Hz, 1H), 4.15 (s, 3H), 3.99 ppm (s, 3H); UV/Vis (EtOH): λ_{max} (ε) = 559 nm (39000 $M^{-1}cm^{-1}$); HR-ESIMS: *m*/*z* calcd for $C_{20}H_{21}N_4$: 317.17607 $[M-CF_3SO_3]^+$; found: 317.17581.

Method B: A solution of *p*-toluenesulfonic acid (few mg) in EtOH (3 mL) was added dropwise to a solution of **11**[10b] (0.256 g, 0.68 mmol) and *N*-phenylhydrazine (0.076 g, 0.70 mmol) in EtOH (20 mL). After stirring overnight at room temperature the solvent was partially removed and the precipitate collected to give the product (0.156 g, 0.33 mmol, 48 %).

2-(*N*,*N*-Diphenylhydrazonomethyl)-*N*-methyl-5-[2-(pyrid-4-yl)vinyl]pyrrole (10b): A mixture of *N*,*N*-diphenylhydrazine hydrochloride (0.520 g, 2.36 mmol) and aldehyde **9**[10c] (0.250 g, 2.36 mmol) in EtOH (5 mL) was heated in a microwave oven under stirring (150 W, 15 min). The deep violet solid was collected by filtration and washed with H_2O (15 mL) to give **10b**·HCl (0.712 g, 1.72 mmol); ^{1}H NMR (500 Hz, [D$_6$]DMSO): $\delta =$ 8.67 (d, $J = 6.2$ Hz, 2H), 8.10 (d, $J = 6.1$ Hz, 2H), 7.95 (d, $J = 15.7$ Hz, 1H), 7.44 (t, $J = 7.7$ Hz, 4H), 7.23 (t, $J = 7.1$ Hz, 2H), 7.18–7.05 (m, 6H), 6.97 (d, $J = 4.1$ Hz, 1H), 6.51 (d, $J = 4.0$ Hz, 1H), 4.00 ppm (s, 3H). The product **10b** was obtained by eluting a solution of its hydrochloride in MeOH through basic Amberlite and upon removal of the solvent under reduced pressure (0.336 g, 0.89 mmol, 38 %). The compound was used in the subsequent step without any further purification.

2-(*N*,*N*-Diphenylhydrazonomethyl)-*N*-methyl-5-[2-(*N*-methylpyrid-4-yl)-vinyl]pyrrole triflate (1b)

Method A: A solution of methyl triflate (0.150 g, 0.91 mmol) in anhydrous CH_3CN (2 mL) was added dropwise to a solution of **10b** (0.266 g, 0.70 mmol) in the same solvent (45 mL). After stirring overnight the solvent was evaporated under reduced pressure to give the product as a deep violet solid (0.140 g, 0.26 mmol, 37 %): M.p. 275 °C (EtOH); ^{1}H NMR (500 MHz, [D$_6$]DMSO): $\delta = 8.67$ (d, $J = 6.6$ Hz, 2H), 8.10 (d, $J = 6.6$ Hz, 2H), 7.96 (d, $J = 15.7$ Hz, 1H), 7.48 (t, $J = 7.8$ Hz, 4H), 7.24 (t, $J = 7.4$ Hz, 2H), 7.20–7.10 (m, 6H), 6.97 (d, $J = 4.2$ Hz, 1H), 6.55 (d, $J = 4.2$ Hz, 1H), 4.17 (s, 3H), 3.99 ppm (s, 3H); UV/Vis (DMSO): λ_{max} (ε) = 528 nm, (40100 $M^{-1}cm^{-1}$); HR-ESIMS: *m*/*z* calcd for $C_{26}H_{25}N_4$: 393.20737 $[M-CF_3SO_3]^+$; found: 393.20704.

Method B: A suspension of *N*,*N*-diphenylhydrazine hydrochloride (0.154 g, 0.70 mmol) in EtOH (5 mL) was added dropwise to a solution of **11**[10b] (0.256 g, 0.68 mmol) in EtOH (20 mL). After stirring for 4 h at room temperature the solvent was partially removed to give the product as a precipitate, which was collected by filtration (0.180 mg, 0.33 mmol, 48 %).

2-(2,4-Dinitrostyryl)-*N*-methylpyrrole (12): Piperidine (6 mL) was added to a solution of 2,4-dinitrotoluene (1.00 g, 5.50 mmol) and *N*-methylpyrrole-2-carbaldehyde (1.20 g, 11.0 mmol) in toluene (20 mL). After stirring for 6 h at 80 °C the red precipitate was collected by filtration and washed with hexane to yield the product as a red solid (0.870 g, 3.19 mmol, 58 %). M.p. 176 °C; ^{1}H NMR (500 MHz, [D$_6$]DMSO): $\delta = 8.70$ (d, $J = 2.4$ Hz, 1H), 8.41 (dd, $J = 9.0$, 2.4 Hz, 1H), 8.33 (d, $J = 9.0$ Hz, 1H), 7.61 (d, $J = 15.8$ Hz, 1H), 7.15 (d, $J = 15.8$ Hz, 1H), 6.99 (dd, $J = 2$,1, 1.8 Hz, 1H), 6.70 (dd, $J = 3.9$, 1.5 Hz, 1H), 6.15 (dd, $J = 3.6$, 2.7 Hz, 1H), 3.78 ppm (s, 3H).

5-(2,4-Dinitrostyryl)-*N*-methylpyrrole-2-carbaldehyde (13): Freshly distilled $POCl_3$ (1.41 g, 9.23 mmol) was added dropwise to anhydrous DMF (0.67 g, 9.2 mmol) at −20 °C under a dry atmosphere. The resulting solution was stirred at 0 °C until a glassy white solid was obtained, which was dissolved in anhydrous CH_3CN (3 mL). A suspension of **12** (1.80 g, 6.59 mmol) in anhydrous CH_3CN (200 mL) was added dropwise to the resulting mixture at 0 °C over a period of 15 min. After stirring overnight at room temperature, the reaction mixture was poured into a 10 % aqueous solution of K_2CO_3 (100 mL) and, after 1 h, the red precipitate was collected by filtration and washed with H_2O (100 mL) to give the product as a red solid (1.51 g, 5.01 mmol, 76 %). M.p. 199 °C; ^{1}H NMR (500 MHz, [D$_6$]DMSO): $\delta = 9.59$ (s, 1H), 8.76 (d, $J = 2.4$ Hz, 1H), 8.52 (dd, $J = 6.2$, 2.6 Hz, 1H), 8.41 (d, $J = 8.8$ Hz, 1H), 7.72 (d, $J = 15.9$ Hz, 1H), 7.53 (d, $J = 15.9$ Hz, 1H), 7.11 (d, $J = 4.4$ Hz, 1H), 6.88 (d, $J = 4.2$ Hz, 1H), 4.07 ppm (s, 3H).

5-(2,4-Dinitrostyryl)-*N*-methyl-2-[(*N*-phenylhydrazono)methyl]pyrrole (2a): *p*-Toluenesulfonic acid (few mg) has been added to a mixture of *N*-

phenylhydrazine (0.029 g, 0.26 mmol) and aldehyde **13** (0.80 g, 0.26 mmol) in EtOH (10 mL). After heating at reflux for 4 h the mixture was poured into a saturated aqueous solution of K_2CO_3 (20 mL) and extracted with CH_2Cl_2 (3×15 mL). The organic layers were combined, dried and evaporated to dryness to leave the product as a violet solid (0.070 g, 0.18 mmol, 69 %). M.p. 230 °C; ^{1}H NMR (500 MHz, [D$_6$]DMSO): $\delta = 10.27$ (s, 1H), 8.70 (d, $J = 2.0$ Hz, 1H), 8.43 (dd, $J = 9.0$, 2.0 Hz, 1H), 8.38 (d, $J = 9.0$ Hz, 1H), 7.88 (s, 1H), 7.70 (d, $J = 15.7$ Hz, 1H), 7.27 (d, $J = 15.7$ Hz, 1H), 7.23 (t, $J = 7.8$ Hz, 2H), 7.01 (d, $J = 8.0$ Hz, 2H), 6.83 (d, $J = 4.1$ Hz, 1H), 6.75 (t, $J = 7.5$ Hz, 1H), 6.53 (d, $J = 4.2$ Hz, 1H), 4.02 ppm (s, 3H); UV/Vis (DMSO): λ_{max} (ε) = 554 nm, (24 000 $M^{-1}cm^{-1}$); HR-ESIMS: m/z calcd for $C_{20}H_{17}N_5O_4Na$: 414.11728 $[M+Na]^+$; found: 414.11746.

5-(2,4-Dinitrostyryl)-*N*-methyl-2-[(*N*,*N*-diphenylhydrazono)methyl]pyrrole (2b): A mixture of *N*,*N*-diphenylhydrazine hydrochloride (0.220 g, 1.00 mmol) and aldehyde **13** (0.300 g, 1.00 mmol) was suspended in EtOH (30 mL) and heated at reflux for 4 h. The solid was collected by filtration and washed with hot H_2O (20 mL) to give the product as a deep violet solid (0.230 g, 0.49 mmol, 49 %). M.p. 193 °C; ^{1}H NMR (500 MHz, [D$_6$]DMSO): $\delta = 8.71$ (d, $J = 2.4$ Hz, 1H), 8.43 (dd, $J = 9.0$, 2.5 Hz, 1H), 8.39 (d, $J = 9.0$ Hz, 1H), 7.70 (d, $J = 15.5$ Hz, 1H), 7.49 (t, $J = 7.9$ Hz, 4H), 7.27 (d, $J = 15.5$ Hz, 1H), 7.23 (t, $J = 7.4$ Hz, 2H), 7.15 (d, $J = 6.5$ Hz, 4H), 7.14 (s, 1H), 6.80 (d, $J = 4.2$ Hz, 1H), 6.46 (d, $J = 4.2$ Hz, 1H), 4.01 ppm (s, 3H); UV/Vis (DMSO) λ_{max} (ε) = 548 nm, (26 000 $M^{-1}cm^{-1}$); HR-ESIMS: m/z calcd for $C_{26}H_{21}N_5O_4Na$: 490.14858 $[M+Na]^+$; found: 490.14893.

5-[(*N*,*N*-Diphenylhydrazono)methyl]-*N*-methylpyrrole-2-carbaldehyde (15): Freshly distilled $POCl_3$ (0.62 g, 4.0 mmol) was added dropwise to anhydrous DMF (0.31 mL) under a dry atmosphere at −10 °C. After 30 min the glassy solid that formed was dissolved in dry 1,2-dichloroethane (20 mL). A solution of **14**[17] (1.00 g, 3.66 mmol) in dry 1,2-dichloroethane (20 mL) at room temperature was then added dropwise. After stirring overnight at room temperature, the reaction mixture was treated with CH_2Cl_2 (20 mL) and poured into a saturated aqueous solution of K_2CO_3 (100 mL). The organic layer was separated, dried and evaporated to dryness to leave a dark-yellow oily residue which was filtrated through silica gel (CH_2Cl_2). The solvent was removed under reduced pressure to give the product as a yellow solid (1.05 g, 3.46 mmol, 95 %): mp 104 °C;[34] ^{1}H NMR ([D$_6$]DMSO) δ 9.52 (s, 1H), 7.49 (t, 4H, $J = 7.8$), 7.26 (t, 2H, $J = 7.4$), 7.17 (d, 4H, $J = 8.0$), 7.15 (s, 1H), 7.02 (d, 1H, $J = 4.2$), 6.55 (d, 1H, $J = 4.2$), 4.08 ppm (s, 3H).

5-[2-(3-Cyano-2-dicyanomethylene-5,5-dimethyl-2,5-dihydrofuran-4-yl)-vinyl]-2-(*N*,*N*-diphenylhydrazonomethyl)-*N*-methylpyrrole—Isomer A (3b-isomer A): A solution of $AcONH_4$ (7 mg) and AcOH (20 mg) in EtOH (1 mL) was added to a solution of aldehyde **15** (1.10 g, 3.62 mmol) and 3-cyano-2-dicyanomethylene-4,5,5-trimethyl-2,5-dihydrofuran[16f] (0.722 g, 3.62 mmol) in the same solvent (130 mL). After stirring for 18 h at 60 °C, the green precipitate was isolated by filtration and washed with hot H_2O (20 mL) to afford the product as a green solid (0.770 g, 1.59 mmol, 44 %). M.p. 270 °C (d); ^{1}H NMR (500 MHz, [D$_6$]DMSO): $\delta = 7.99$ (d, $J = 15.5$ Hz, 1H), 7.53 (d, $J = 4.7$ Hz, 1H), 7.52 (t, $J = 7.5$ Hz, 4H), 7.30 (t, $J = 7.4$ Hz, 2H), 7.21 (d, $J = 7.8$ Hz, 4H), 7.16 (s, 1H), 6.86 (d, $J = 15.5$ Hz, 1H), 6.84 (d, $J = 4.7$ Hz, 1H), 3.89 (s, 3H), 1.72 ppm (s, 6H); UV/Vis (DMSO) λ_{max} (ε) = 656 nm, (63 900 $M^{-1}cm^{-1}$); HR-ESIMS m/z calcd for $C_{30}H_{24}N_6ONa$: 507.19038 $[M+Na]^+$; found: 507.19091.

5-[2-(3-Cyano-2-dicyanomethylene-5,5-dimethyl-2,5-dihydrofuran-4-yl)-vinyl]-2-(*N*,*N*-diphenylhydrazonomethyl)-*N*-methylpyrrole—Isomer B (3b-isomer B): A mixture of aldehyde **15** (1.05 g, 3.46 mmol) and 3-cyano-2-dicyanomethylene-4,5,5-trimethyl-2,5-dihydrofuran[16f] (0.689 g, 3.46 mmol) in EtOH (20 mL) was heated at reflux under microwave conditions in an open vessel at a constant power of 40 W for 15 min with simultaneous cooling and stirring. After cooling to 0 °C the precipitate was collected by filtration to give the product as a deep-blue solid (1.10 g, 2.27 mmol, 66 %). M.p. 251–252 °C; ^{1}H NMR (500 MHz, [D$_6$]DMSO): $\delta = 7.86$ (d, $J = 15.5$ Hz, 1H), 7.51 (t, $J = 7.8$ Hz, 4H), 7.32 (s, 1H), 7.28 (t, $J = 7.4$ Hz, 2H), 7.18 (d, $J = 6.7$ Hz, 4H), 7.12 (d, $J = 2.8$ Hz, 1H), 6.84 (d, $J = 2.8$ Hz, 1H), 6.73 (d, $J = 15.5$ Hz, 1H), 3.83 (s, 3H), 1.61 ppm (s, 6H); UV/Vis (DMSO) λ_{max} (ε) = 596 nm, ((26 600 ± 900) $M^{-1}cm^{-1}$); HR-ESIMS: m/z calcd for $C_{30}H_{24}N_6ONa$: 507.19038 $[M+Na]^+$; found: 507.19117.

Semiempirical calculations: Geometries have been fully optimised using the PM3 Hamiltonian as available in the Gaussian 03 program package.[35] Different structures have been used as starting geometries. Optimisation was carried out with no symmetry constraints.

EOA measurements: All EOA and UV/Vis spectra were recorded in anhydrous 1,4-dioxane prepared by distillation from Na under Argon prior to use. The UV/Vis spectra required for the evaluation of the integral absorption, band maxima and the first $[t(\tilde{\nu})]$ and second $[u(\tilde{\nu})]$derivatives of the optical absorption spectrum were recorded with a Perkin–Elmer Lambda 900 spectrophotometer at 298 K (scan speed of 50 nm min^{-1}; 3 cm quartz glass cuvette). The EOA signal has been recorded with an integration time of 0.5–1 min (depending on the quality of the signal) and *p*-amino-*p*′-nitrobiphenyl was used as a calibrating reference. From multilinear fittings of $L\varepsilon\tilde{\nu}^{-1}$ as a function of the first $[t(\tilde{\nu})]$ and second $[u(\tilde{\nu})]$ derivatives of the optical absorption spectrum five parameters, *E*, *D*, *F*, *G*, *H* and *I*, can be obtained and are the basis for the evaluations of the dipole moments μg and $\Delta\mu = \mu_e - \mu g$ and by this μ_e along the transition dipole moment direction.

Thermal stability studies of compounds 1b–3b: Cast or spin-coated films on glass substrates of host-guest polymer composites were prepared by doping commercial polysulfone (Aldrich, average M_n ca. 22 000) with 50 wt % chromophore. Films were heated at 100, 120, 140, 160, 180 and 200 °C for 20 min at each temperature value in the air. Thermal degradation of the chromophore in the host polymeric matrix was monitored by measuring the decrease of the UV/Vis absorption at λ_{max}.

Acknowledgements

Research was supported by the European Commission through NMP3-CT-2003-505478 contract (STRP-ODEON) and MIUR-FIRB RBNE033KMA (Molecular compounds and hybrid nanostructured materials with resonant and non-resonant optical properties for photonic devices).

---

[1] a) *Molecular Nonlinear Optics* (Ed.: J. Zyss), Academic Press, New York, **1994**; b) "Optical Nonlinearities in Chemistry": *Chem. Rev.* **1994**, *94*, 1–278, edited by D. M. Burland; c) P. N. Prasad, D. J. Williams, *Introduction to Nonlinear Optical Effects in Molecules and Polymers*, Wiley, New York, **1991**.

[2] For reviews, see: a) L. R. Dalton, *J. Phys. Condens. Matter* **2003**, *15*, R897–R934; b) H. Ma, A. K. Y. Jen, L. R. Dalton, *Adv. Mater.* **2002**, *14*, 1339–1365; c) H. Ma, S. Liu, J. Luo, S. Suresh, L. Liu, S. H. Kang, M. Haller, T. Sassa, L. R. Dalton, A. K. Y. Jen, *Adv. Funct. Mater.* **2002**, *12*, 565–574; d) M. E. van der Boom, *Angew. Chem.* **2002**, *114*, 3511–3514; *Angew. Chem. Int. Ed.* **2002**, *41*, 3363–3366; e) L. R. Dalton, W. H. Steier, B. H. Robinson, C. Zhang, A. Ren, S. Garner, A. T. Chen, T. Londergan, L. Irwin, B. Carlson, L. Fifield, G. Phelan, C. Kincaid, J. Amend, A. Jen, *J. Mater. Chem.* **1999**, *9*, 1905–1920; f) T. Verbiest, M. Kauranen, A. Persoons, *J. Mater. Chem.* **1999**, *9*, 2005–2012; g) J. J. Wolff, R. Wortmann, *J. Prakt. Chem./Chem.-Ztg.* **1998**, *340*, 99–111; h) S. R. Marder, B. Kippelen, A. K. Y. Jen, N. Peyghambarian, *Nature* **1997**, *388*, 845–851.

[3] For some recent examples, see: a) J. A. Davies, A. Elangovan, P. A. Sullivan, B. C. Olbricht, D. H. Bale, T. R. Ewy, C. M. Isborn, B. E. Eichinger, B. H. Robinson, P. J. Reid, X. Li, L. R. Dalton, *J. Am. Chem. Soc.* **2008**, *130*, 10565–10575; b) M. Halter, Y. Liao, R. M. Plocinik, D. C. Coffey, S. Bhattacharjee, U. Mazur, G. J. Simpson, B. H. Robinson, S. L. Keller, *Chem. Mater.* **2008**, *20*, 1778–1787; c) S. R. Hammond, O. Clot, K. A. Firestone, D. H. Bale, D. Lao, M. Haller, G. D. Phelan, B. Carlson, A. K. Y. Jen, P. J. Reid, L. R. Dalton, *Chem. Mater.* **2008**, *20*, 3425–3434; d) Z. Shi, J. Luo, S. Huang, X. H. Zhou, T. D. Kim, Y. J. Cheng, B. M. Polishak, T. R. Younkin, B. A. Block, A. K. Y. Jen, *Chem. Mater.* **2008**, *20*, 6372–

6377; e) Y. Xiong, H. Tang, J. Zhang, Z. Y. Wang, J. Campo, W. Wenseleers, E. Goovaerts, *Chem. Mater.* **2008**, *20*, 7465–7473; f) C.-Z. Zhang, C. Lu, J. Zhu, C. Y. Wang, G.-Y. Lu, C.-S. Wang, D.-L. Wu, F. Liu, Y. Cui, *Chem. Mater.* **2008**, *20*, 4628–4641; g) Y. J. Cheng, J. Luo, S. Hau, D. H. Bale, T. D. Kim, Z. Shi, D. B. Lao, N. M. Tucker, Y. Tian, L. R. Dalton, P. J. Reid, A. K.-Y. Jen, *Chem. Mater.* **2007**, *19*, 1154–1163.

[4] For electro-optic modulators, see: a) Y. G. Zhao, A. Wu, H. L. Lu, S. Chang, W. K. Lu, S. T. Ho, M. E. van der Boom, T. J. Marks, *Appl. Phys. Lett.* **2001**, *79*, 587–589.

[5] *Comprehensive Heterocyclic Chemistry* (Eds.: A. R. Katritzky, C. W. Rees), Pergamon Press, Oxford, **1984**.

[6] a) M. M. M. Raposo, A. M. R. C. Sousa, G. Kirsch, P. Cardoso, M. Belsley, E. De Matos Gomes, A. M. C. Fonseca, *Org. Lett.* **2006**, *8*, 3681–3684; b) I. D. L. Albert, T. J. Marks, M. A. Ratner, *Chem. Mater.* **1998**, *10*, 753–762; c) P. R. Varanasi, A. K. Y. Jen, J. Chandrasekhar, I. N. N. Namboothiri, A. Rathna, *J. Am. Chem. Soc.* **1996**, *118*, 12443–12448.

[7] a) M. G. Hutchings, I. Ferguson, D. J. McGeein, J. O. Morley, J. Zyss, I. Ledoux, *J. Chem. Soc. Perkin Trans. 2* **1995**, 171–176; b) P. Boldt, T. Eisentraeger, C. Glania, J. Goeldenitz, P. Kraemer, R. Matschiner, J. Rase, R. Schwesinger, J. Wichern, R. Wortmann, *Adv. Mater.* **1996**, *8*, 672–675.

[8] A. Facchetti, E. Annoni, L. Beverina, M. Morone, P. Zhu, T. J. Marks, G. A. Pagani, *Nat. Mater.* **2004**, *3*, 910–917.

[9] a) A. Abbotto, S. Bradamante, A. Facchetti, G. A. Pagani, *J. Org. Chem.* **1997**, *62*, 5755–5765; b) S. Bradamante, A. Facchetti, G. A. Pagani, *J. Phys. Org. Chem.* **1997**, *10*, 514–524; c) A. Abbotto, S. Bradamante, G. A. Pagani, *J. Org. Chem.* **2001**, *66*, 8883–8892; d) A. Abbotto, L. Beverina, S. Bradamante, A. Facchetti, C. Klein, G. A. Pagani, M. Redi-Abshiro, R. Wortmann, *Chem. Eur. J.* **2003**, *9*, 1991–2007; e) G. Archetti, A. Abbotto, R. Wortmann, *Chem. Eur. J.* **2006**, *12*, 7151–7160.

[10] a) A. Abbotto, L. Beverina, R. Bozio, S. Bradamante, C. Ferrante, G. A. Pagani, R. Signorini, *Adv. Mater.* **2000**, *12*, 1963–1967; b) A. Abbotto, L. Beverina, R. Bozio, A. Facchetti, C. Ferrante, G. A. Pagani, D. Pedron, R. Signorini, *Org. Lett.* **2002**, *4*, 1495–1498; c) A. Abbotto, L. Beverina, R. Bozio, A. Facchetti, C. Ferrante, G. A. Pagani, D. Pedron, R. Signorini, *Chem. Commun.* **2003**, 2144–2145.

[11] I. D. L. Albert, T. J. Marks, M. A. Ratner, *J. Am. Chem. Soc.* **1997**, *119*, 6575–6582.

[12] L. Beverina, J. Fu, A. Leclercq, E. Zojer, P. Pacher, S. Barlow, E. W. Van Stryland, D. J. Hagan, J.-L. Bredas, S. R. Marder, *J. Am. Chem. Soc.* **2005**, *127*, 7282–7283.

[13] E. Barchiesi, S. Bradamante, C. Carfagna, R. Ferraccioli, *J. Chem. Soc. Perkin Trans. 2* **1988**, 1565–1572.

[14] B. G. Tiemann, S. R. Marder, J. W. Perry, L. T. Cheng, *Chem. Mater.* **1990**, *2*, 690–695.

[15] G. Melikian, F. P. Rouessac, C. Alexandre, *Synth. Commun.* **1995**, *25*, 3045–3051.

[16] a) S. Gilmour, R. A. Montgomery, S. R. Marder, L. T. Cheng, A. K. Y. Jen, Y. M. Cai, J. W. Perry, L. R. Dalton, *Chem. Mater.* **1994**, *6*, 1603–1604; b) F. Wang, A. S. Ren, M. He, A. W. Harper, L. R. Dalton, S. M. Garner, H. Zhang, A. Chen, W. H. Steier, *Polym. Mater. Sci. Eng.* **1998**, *78*, 42; c) B. H. Robinson, L. R. Dalton, A. W. Harper, A. Ren, F. Wang, C. Zhang, G. Todorova, M. Lee, R. Aniszfeld, S. Garner, A. Chen, W. H. Steier, S. Houbrecht, A. Persoons, I. Ledoux, J. Zyss, A. K. Y. Jen, *Chem. Phys.* **1999**, *245*, 35–50; d) C. Zhang, A. S. Ren, F. Wang, J. Zhu, L. R. Dalton, J. N. Woodford, C. H. Wang, *Chem. Mater.* **1999**, *11*, 1966–1968; e) C. Zhang, L. R. Dalton, M.-C. Oh, H. Zhang, W. H. Steier, *Chem. Mater.* **2001**, *13*, 3043–3050; f) S. Liu, M. A. Haller, H. Ma, L. R. Dalton, S. H. Jang, A. K. Y. Jen, *Adv. Mater.* **2003**, *15*, 603–607.

[17] L. Beverina, A. Abbotto, M. Landenna, M. Cerminara, R. Tubino, F. Meinardi, S. Bradamante, G. A. Pagani, *Org. Lett.* **2005**, *7*, 4257–4260.

[18] O. Kwon, S. Barlow, S. A. Odom, L. Beverina, N. J. Thompson, E. Zojer, J.-L. Bredas, S. R. Marder, *J. Phys. Chem. A* **2005**, *109*, 9346–9352.

[19] C. Reichardt, *Solvent Effects in Organic Chemistry*, VCH, Weinheim, **1979**, Chapter 6.

[20] J. L. Oudar, D. S. Chemla, *J. Chem. Phys.* **1977**, *66*, 2664–2668.

[21] a) W. Liptay in *Excited States, Vol. 1, Dipole Moments and Polarizabilities of Molecules in Excited Electronic States* (Ed.: E. C. Lim), Academic Press, New York, **1974**, pp. 129–229; b) R. Wortmann, K. Elich, S. Lebus, W. Liptay, P. Borowicz, A. Grabowska, *J. Phys. Chem.* **1992**, *96*, 9724–9730.

[22] a) S. Beckmann, K.-H. Etzbach, P. Krämer, K. Lukaszuk, R. Matschiner, A. J. Schmidt, P. Schumacher, R. Sens, G. Seibold, R. Wortmann, F. Würthner, *Adv. Mater.* **1999**, *11*, 536–541; b) F. Würthner, C. Thalacker, R. Matschiner, K. Lukaszuk, R. Wortmann, *Chem. Commun.* **1998**, 1739–1740.

[23] F. Steybe, F. Effenberger, P. Kramer, C. Glania, R. Wortmann, *Chem. Phys.* **1997**, *219*, 317–331.

[24] C. J. F. Böttcher, *Theory of Electric Polarization: Dielectrics in Static Fields*, Elsevier, Amsterdam, **1973**.

[25] J. J. Wolff, R. Wortmann, *Adv. Phys. Org. Chem.* **1999**, *32*, 121–217.

[26] a) R. Wortmann, C. Poga, R. J. Twieg, C. Geletneky, C. R. Moylan, P. M. Lundquist, R. G. DeVoe, P. M. Cotts, H. Horn, J. E. Rice, D. M. Burland, *J. Chem. Phys.* **1996**, *105*, 10637–10647; b) A. Willetts, J. E. Rice, D. M. Burland, D. P. Shelton, *J. Chem. Phys.* **1992**, *97*, 7590–7599.

[27] S. Stadler, G. Dietrich, G. Bourhill, C. Bräuchle, A. Pawlik, W. Grahn, *Chem. Phys. Lett.* **1995**, *247*, 271.

[28] Paralite Optical Parametrical Oscillator, LAS GmbH.

[29] T. Kodaira, A. Watanabe, O. Ito, M. Matsuda, K. Clays, A. Persoons, *J. Chem. Soc. Faraday Trans.* **1997**, *93*, 3039.

[30] C. Lambert, G. Nöll, E. Schmälzlin, K. Meerholz, C. Bräuchle, *Chem. Eur. J.* **1998**, *4*, 2129.

[31] C. Lambert, W. Gaschler, E. Schmälzlin, K. Meerholz, C. Bräuchle, *J. Chem. Soc. Perkin Trans. 2* **1999**, 577.

[32] The poling of host–guest and side-chain polymers and sol–gel materials is under investigation and will be reported in due course.

[33] M. Goebel, Dissertation, Kaiserslautern (Germany), **2006**.

[34] When the reaction mixture was heated at reflux for 2 h instead of being stirred overnight at room temperature and then treated in the same manner, the product was obtained as a dark-yellow oil in a yield of 95% and identified as a mixture of two isomers, one of which was the same as the yellow solid obtained in the first procedure; ^{1}H NMR (500 MHz, [D$_6$]DMSO) of the second isomer: $\delta=$ 9.72 (s, 1H), 7.70 (s, 1H), 7.50 (t, $J=7.5$ Hz, 4H), 7.25 (t, $J=7.3$ Hz, 2H), 7.17 (d, $J=8.1$ Hz, 4H), 6.98 (d, $J=3.0$ Hz, 1H), 6.52 (d, $J=3.4$ Hz, 1H), 3.92 ppm (s, 3H).

[35] Gaussian 03, Revision B.05, M. J. Frisch, G. W. Trucks, H. B. Schlegel, G. E. Scuseria, M. A. Robb, J. R. Cheeseman, J. A. Montgomery, Jr., T. Vreven, K. N. Kudin, J. C. Burant, J. M. Millam, S. S. Iyengar, J. Tomasi, V. Barone, B. Mennucci, M. Cossi, G. Scalmani, N. Rega, G. A. Petersson, H. Nakatsuji, M. Hada, M. Ehara, K. Toyota, R. Fukuda, J. Hasegawa, M. Ishida, T. Nakajima, Y. Honda, O. Kitao, H. Nakai, M. Klene, X. Li, J. E. Knox, H. P. Hratchian, J. B. Cross, C. Adamo, J. Jaramillo, R. Gomperts, R. E. Stratmann, O. Yazyev, A. J. Austin, R. Cammi, C. Pomelli, J. W. Ochterski, P. Y. Ayala, K. Morokuma, G. A. Voth, P. Salvador, J. J. Dannenberg, V. G. Zakrzewski, S. Dapprich, A. D. Daniels, M. C. Strain, O. Farkas, D. K. Malick, A. D. Rabuck, K. Raghavachari, J. B. Foresman, J. V. Ortiz, Q. Cui, A. G. Baboul, S. Clifford, J. Cioslowski, B. B. Stefanov, G. Liu, A. Liashenko, P. Piskorz, I. Komaromi, R. L. Martin, D. J. Fox, T. Keith, M. A. Al-Laham, C. Y. Peng, A. Nanayakkara, M. Challacombe, P. M. W. Gill, B. Johnson, W. Chen, M. W. Wong, C. Gonzalez, J. A. Pople, Gaussian, Inc., Pittsburgh PA, **2003**.

Received: February 3, 2009